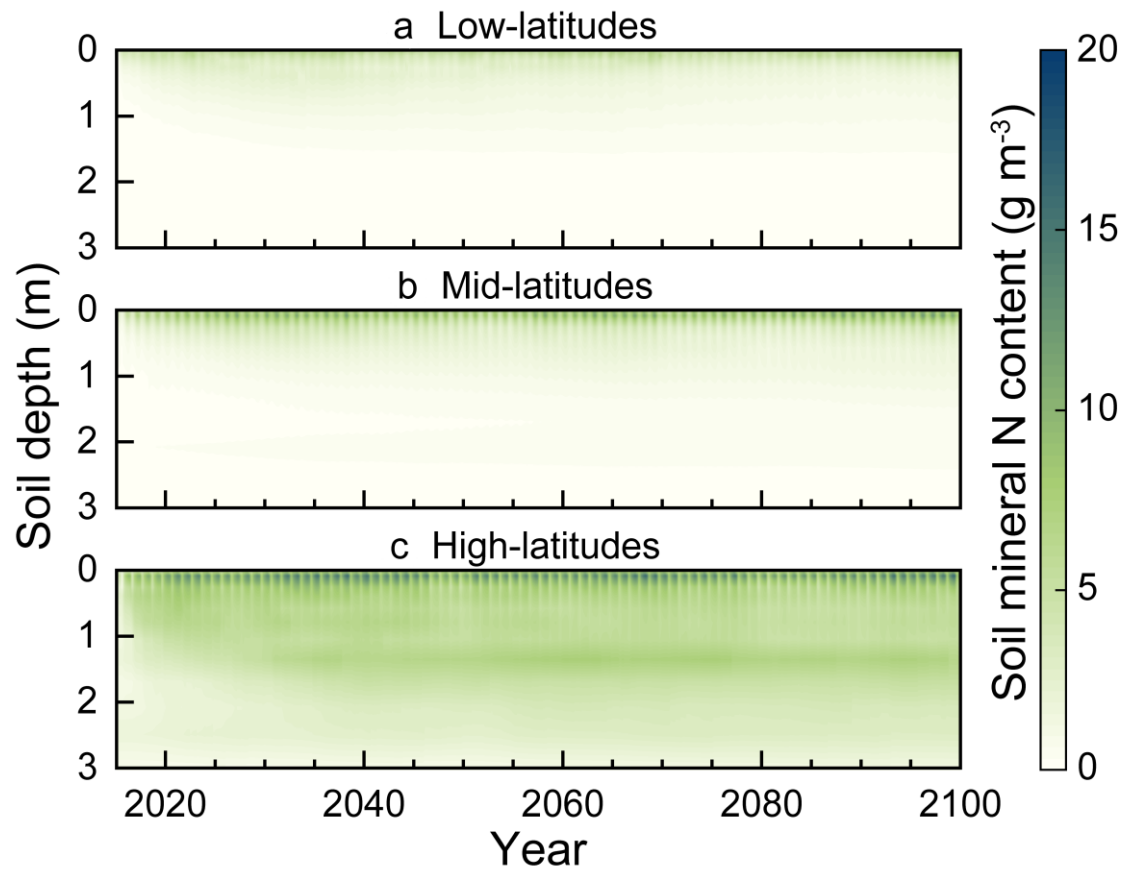
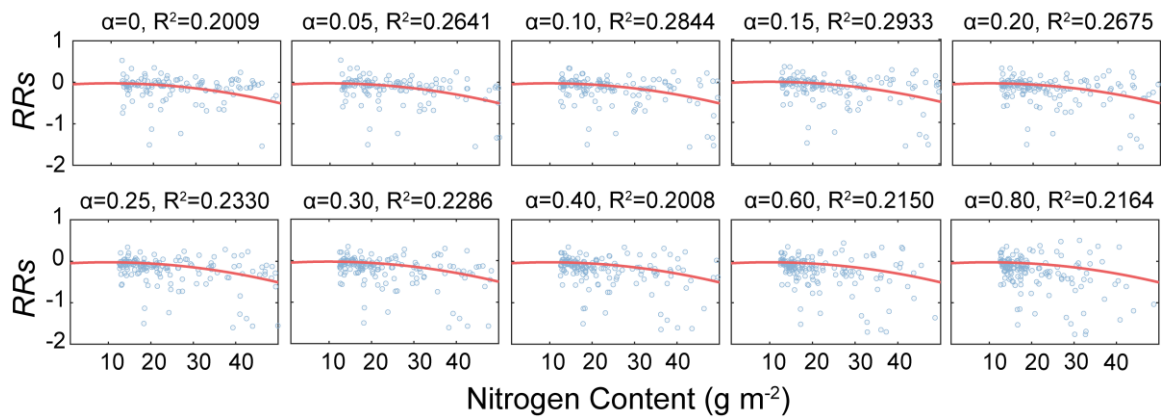


Supplementary figures



**Figure S1 Mineral N content predicted by CLM5 for different soil depths in low-latitudes (a), mid-latitude (b), and high latitudes (c). The majority of soil mineral N is primarily concentrated in the topsoil.**



**Figure S2** The responses of soil respiration ( $Rs$ ) to nitrogen (N) addition ( $RR_s$ ) fitted with N content with different  $\alpha$  values.

10

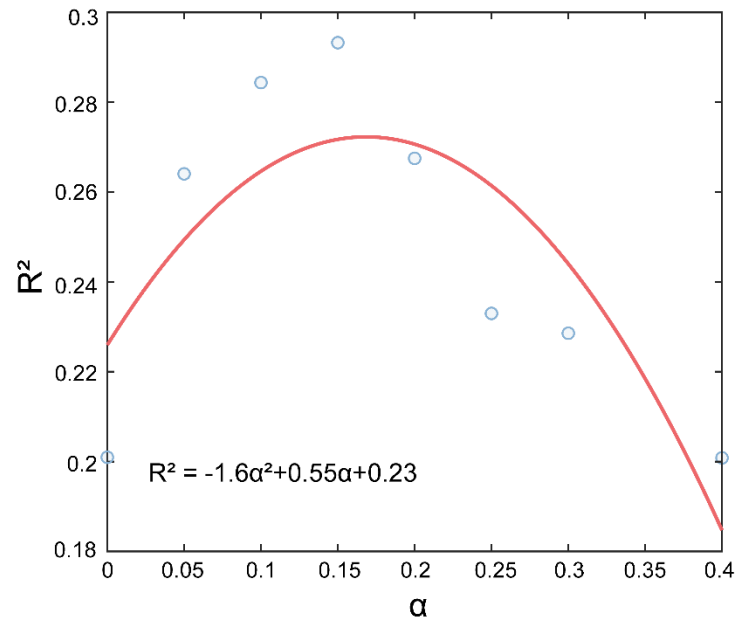
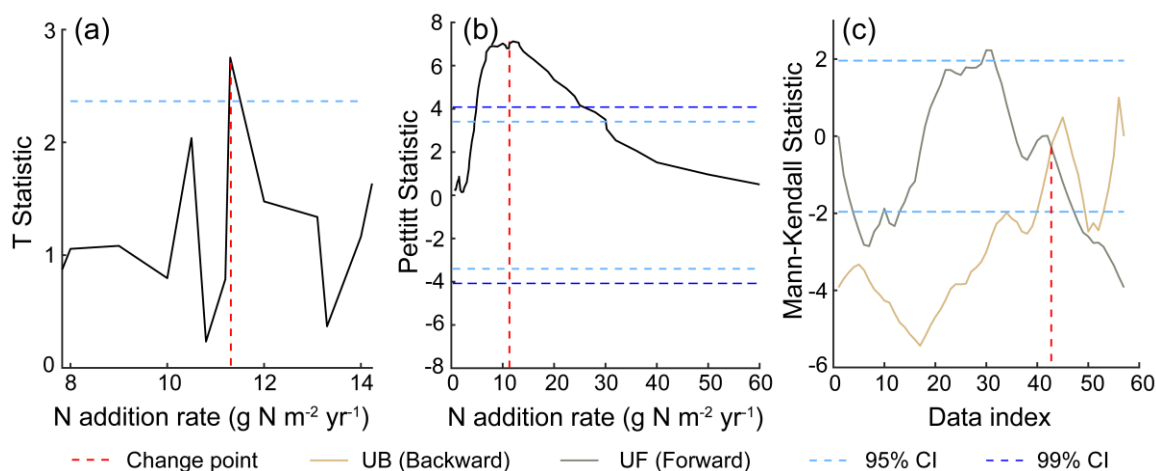


**Figure S3 A quadratic fitting of the  $R^2$  for each test run, searching for the "best" model parameter.** Two extreme  $\alpha$  values (0.6 and 0.8, Fig. S2) were excluded from the curve fitting due to their large deviation from the optimal range, which could have distorted the fitted curve near the peak.

15



20 **Figure S4 The identification of N addition threshold.** (a) Sliding t-test, (b) Pettitt test, and (c) Mann-Kendall test. The x-axis in (c) represents the index sorted by ascending N addition levels, rather than the absolute N addition values. The detected change point corresponds to an N addition level of 14 g N m<sup>-2</sup> yr<sup>-1</sup>. The dark blue and light blue dashed lines represent the 99% and 95% confidence intervals (CIs), respectively.

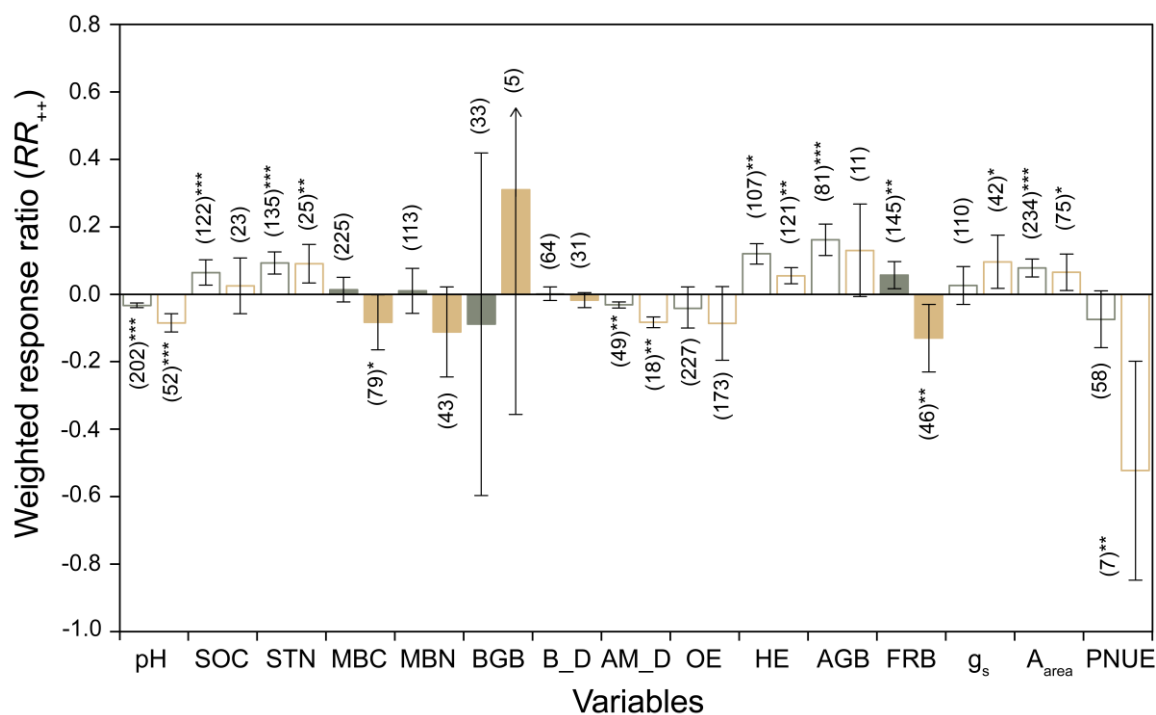


**Figure S5 Weighted response ratios for control variables to low (LN) and high (HN) additions.** N addition rates refer to Fig. 4. The SOC, STN, MBC, MBN, BGB, B\_D, AM\_D, OE, HE, AGB, FRB, g<sub>s</sub>, A<sub>area</sub>, and PNUE represent soil organic carbon, soil total nitrogen, soil microbial biomass carbon, soil microbial biomass nitrogen, belowground biomass, bacterial diversity, arbuscular mycorrhizal fungi diversity, activity of oxidative enzymes, activity of hydrolytic enzymes, aboveground biomass, fine root biomass, stomatal conductance, photosynthetic rate per area, photosynthetic nitrogen use efficiency, respectively. Error bars represent 95% confidence intervals (CIs) for the response ratios. The numbers in parentheses indicate the sample size. Asterisks \*, \*\*, and \*\*\* denote significant effects at  $p < 0.05$ ,  $p < 0.01$ , and  $p < 0.001$ , respectively. The filled and empty bars represent significant differences and no difference between LN and HN, respectively.

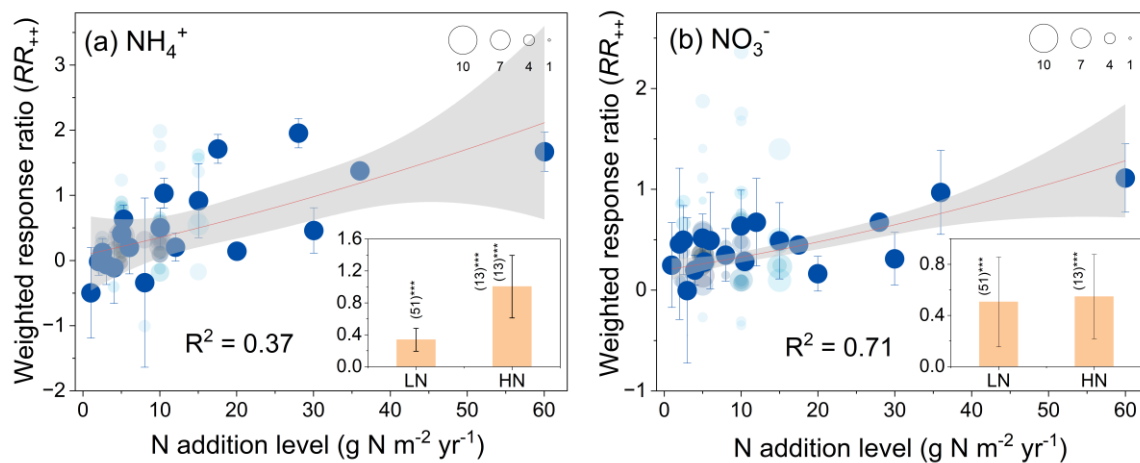


**Figure S6 Weighted responses of (a)  $\text{NH}_4^+$  and (b)  $\text{NO}_3^-$  to N addition along with N-added gradient.** The insets represent the overall effects of  $\text{NH}_4^+$  and  $\text{NO}_3^-$  at low (LN) and high (HN) N additions, respectively. The error bars and shaded areas represent the 95% confidence intervals of  $RR_{++}$  and the fitted curve, respectively.

40

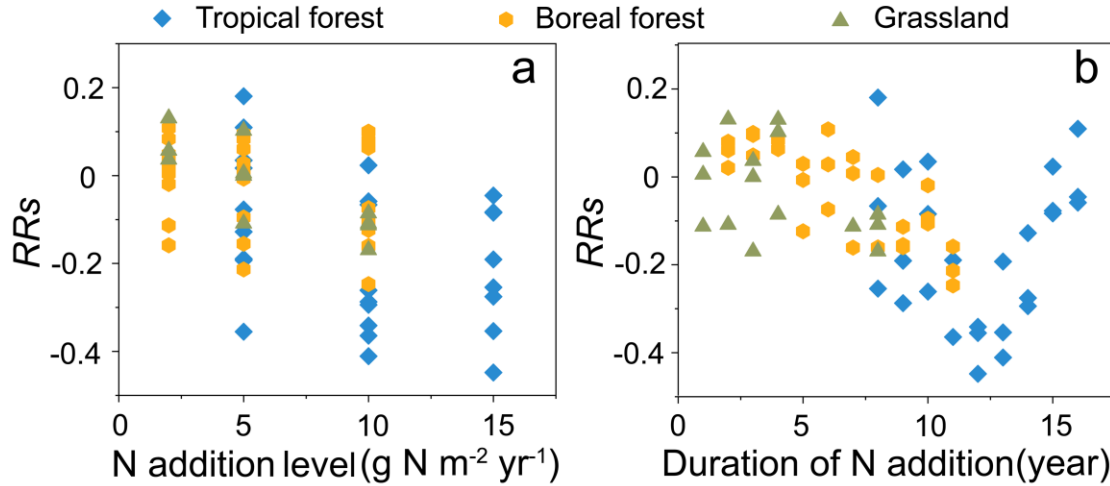


**Figure S7. The changes of  $RR_s$  with N-added gradient (a) and experimental duration of N addition (b).**

We extracted three records of long-term sentinel N-addition experiments from global datasets from tropical forests (Zheng et al., 2022), boreal forests (Xing et al., 2020), and grasslands (Zeng et al., 2020), respectively. In all three ecosystems,  $RR_s$  showed a decreasing trend, implying that soil respiration ( $R_s$ ) began to be inhibited as N addition increases (a). In grasslands,  $R_s$  was completely inhibited at an N addition of  $10 \text{ g N m}^{-2} \text{yr}^{-1}$  (a), which is less than the global-scale N threshold ( $N_{Th}$ ) in this study, whereas in tropical and boreal forests,  $R_s$  was still stimulated at  $10 \text{ g N m}^{-2} \text{yr}^{-1}$  (a), suggesting that  $N_{Th}$  higher than  $10 \text{ g N m}^{-2} \text{yr}^{-1}$  is possible in these ecosystems. Irrespective of N addition, the  $RR_s$  showed a decreasing trend with experimental duration (b). Previous studies have suggested that the  $N_{Th}$  of  $R_s$  exists, while it differs between ecosystems. The inhibitory effect of N on  $R_s$  increased with the accumulation of soil N, further confirming the inhibitory effect of excessive N on  $R_s$ . It is not plausible to determine  $N_{Th}$  for each individual ecosystem due to data unavailability in this study that aimed to explore the impacts on estimation of C-N cycle after considering N thresholds. Therefore, we alternatively derived a universal threshold from the meta-analysis on a global scale. With  $N_{Th}$  imported in the CLM5, the model results also verify that the vast majority of mid- and low-latitude regions do not reach a soil mineral N concentration of  $11.3 \text{ g m}^{-2}$  by 2100 (Fig. 5a, b). The new N scheme acts primarily at high latitudes, in which model uncertainty could also arise primarily. The complex spatial heterogeneity of the N effects on  $R_s$  highlighted the need of further site experiments for more information on the N thresholds under different ecosystems.

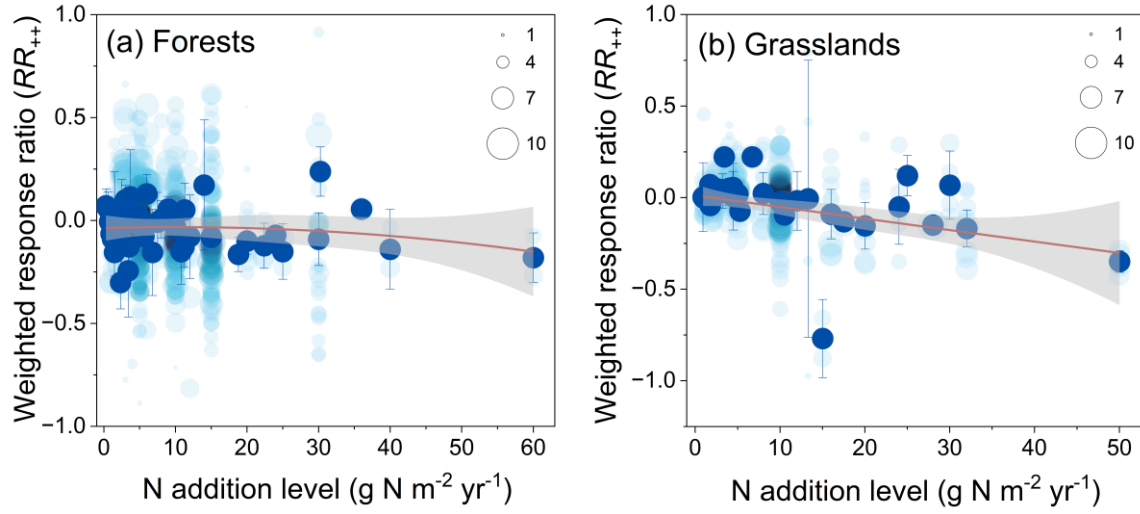


**Figure S8 Weighted response of soil respiration ( $R_s$ ) to N addition along with N-added gradient in (a) forest and (b) grassland ecosystem.** The semi-transparent blue dots represent all observations and the size of the dots represents  $\ln \omega_i$ , and the shade of the dots color indicates the density of the dot distribution. The error bars and shaded areas represent the 95% confidence intervals of  $RR_{++}$  and the fitted curve, respectively.

65



## Supplementary tables

70

**Table S1** Variables used for the meta-analysis

Variable Type	Variables	Variable Abbreviation.
Soil respiration	Total soil respiration	<i>Rs</i>
	Heterotrophic respiration	<i>Rh</i>
	Autotrophic respiration	<i>Ra</i>
Location	Latitude	latitude
	Longitude	longitude
Climate factors	Mean annual temperature	MAT
	Mean annual precipitation	MAP
Soil properties	Soil organic carbon	SOC
	Soil total nitrogen	STN
	Soil microbial biomass carbon	MBC
	Soil microbial biomass nitrogen	MBN
	Aboveground biomass	AGB
Biomass	Belowground biomass	BGB
	Fine root biomass	FBC
Vegetation type	Forest type	temperate, tropical, coniferous, deciduous broad-leaved, evergreen broadleaf
Photosynthetic factor (Liang et al., 2020)	Photosynthetic rate per area	$A_{area}$
	Stomatal conductance	$g_s$
	Photosynthetic nitrogen use efficiency	PNUE
Microbial diversity (Ma et al., 2021 ; Wang et al., 2018)	Bacterial diversity	B_D
	Arbuscular mycorrhizal fungi diversity	AM_D
Enzymatic activity (Fan et al., 2018)	Oxidative enzymes	OE
	Hydrolytic enzymes	HE

**Table S2** The depth of soil layers

Soil layers	Total depth (m)	Layer depth (m)
1	0.01	0.01
2	0.04	0.03
3	0.09	0.05
4	0.16	0.07
5	0.26	0.10
6	0.40	0.14
7	0.58	0.18
8	0.80	0.22
9	1.06	0.26
10	1.36	0.30
11	1.70	0.34
12	2.08	0.38
13	2.50	0.42
14	2.99	0.49
15	3.58	0.59
16	4.27	0.69
17	5.06	0.79
18	5.95	0.89
19	6.94	0.99
20	8.03	1.09
21	9.80	1.77
22	13.33	3.53
23	19.48	6.15
24	28.87	9.39
25	42.00	13.13

**Table S3** Sensitivity cases for CLM5

Case name	Nitrogen decomposition module setting	Simulation period
Historical control case	Original CLM5 ( $\alpha=0$ )	1950-2014
Sensitivity case 1	$\alpha=0.05$	1950-2014
Sensitivity case 2	$\alpha=0.10$	1950-2014
Sensitivity case 3	$\alpha=0.15$	1950-2014
Sensitivity case 4	$\alpha=0.20$	1950-2014
Sensitivity case 5	$\alpha=0.25$	1950-2014
Sensitivity case 6	$\alpha=0.30$	1950-2014
Sensitivity case 7	$\alpha=0.40$	1950-2014
Sensitivity case 8	$\alpha=0.60$	1950-2014
Sensitivity case 9	$\alpha=0.80$	1950-2014
Projection control case	Original CLM5 ( $\alpha=0$ )	2015-2100
Projection threshold case	$\alpha=0.172$	2015-2100

## References

- 80 Zheng, M., Zhang, T., Luo, Y., Liu, X., Ye, Q., Wang, S. et al. (2022). Temporal patterns of soil carbon emission in tropical forests under long-term nitrogen deposition. *Nature Geoscience*, 15, 1002–1010. <https://doi.org/10.1038/s41561-022-01080-4>
- Xing, A., Du, E., Shen, H., Xu, L., Zhang, M., Liu, X. et al. (2020). High-level nitrogen additions accelerate soil respiration reduction over time in a boreal forest. *Ecology Letters*, 25, 1869–1878. <https://doi.org/10.1111/ele.14065>
- 85 Zeng, W., Zhang, J., Dong, L., Wang, W. & Zeng H. (2020). Nonlinear responses of total belowground carbon flux and its components to increased nitrogen availability in temperate forests. *Science of the Total Environment*, 715, 136954. <https://doi.org/10.1016/j.scitotenv.2020.136954>